Engineering with Computers
https://doi.org/10.1007/s00366-020-01026-7

ORIGINAL ARTICLE

Novel solution for heat and mass transfer of a MHD micropolar fluid flow on a moving plate with suction and injection

F. Baharifard[1] · K. Parand[2,3,4] · M. M. Rashidi[5]

Received: 6 January 2020 / Accepted: 16 April 2020

Abstract

Two new functions on the semi-infinite interval, namely Rational Gegenbauer (R) and Exponential Gegenbauer (E) functions are proposed to solve the heat transfer problem. The considered problem is flow of MHD micropolar over a moving plate with suction and injection boundary conditions. For applying Tau method efficiently, two matrices of derivative and product for both of rational and exponential Gegenbauer whose enable us to solve a system of nonlinear algebraic equations on the semi-infinite interval were introduced, and an error bound of these functions approximation was estimated which led to have an exponential convergence rate in this method. Moreover, the influence of the important physical parameters on heat and mass transfer phenomena are studied with details. Comparing the results of Rational Gegenbauer Tau and Exponential Gegenbauer Tau methods with available analytical and numerical solutions shows that the present methods are efficient and have fast convergence rate and high accuracy. This method can solve a set of coupled nonlinear and high-order differential equations on a semi-infinite domain by converting to a set of linear equations.

Keywords Tau method · Rational Gegenbauer functions · Exponential Gegenbauer functions · Magneto-micropolar · Suction and injection · Radiation heat transfer

Mathematics Subject Classification 34B15 · 34B40 · 65L05 · 65L60

List of symbols

b	Constant
B_0	Uniform transverse magnetic field
c_f	Skin-friction coefficient
c_p	Specific heat at constant pressure
Ec	Eckert number
f	Dimensionless velocity
G	Microrotation parameter
g	Dimensionless microrotation
G_1	Microrotation constant
K	Coupling constant parameter
k^*	Mean absorption coefficient
M	Magnetic field parameter
N	Components of microrotation
Nu	Nusselt number
Pr	Prandtl number
q_r	Radiative heat flux
q_w	Surface heat flux
R	Thermal radiation parameter
Re	Reynolds number
s	Constant characteristic of the fluid
T	Temperature of fluid
u, v	Velocity components along x and y directions, respectively

✉ F. Baharifard
f.baharifard@ipm.ir

K. Parand
k_parand@sbu.ac.ir

M. M. Rashidi
mm_rashidi@yahoo.com

[1] School of Computer Science, Institute for Research in Fundamental Sciences (IPM), Tehran, Iran

[2] Department of Computer Sciences, Faculty of Mathematical Sciences, Shahid Beheshti University, G. C., Tehran, Iran

[3] Department of Cognitive Modeling, Institute for Cognitive and Brain Sciences, Shahid Beheshti University, G. C., Tehran, Iran

[4] Department of Statistics and Actuarial Science, University of Waterloo, Waterloo, Canada

[5] Shanghai Key Lab of Vehicle Aerodynamics and Vehicle Thermal Management Systems, Tongji University, 4800 Cao An Rd., Jiading 201804, Shanghai, China

Published online: 21 May 2020

x, y Cartesian coordinates along the plate and normal to it, respectively

Greek symbols

η Similarity variable
γ Constant
κ Thermal conductivity
μ Dynamic viscosity
ν Kinematic viscosity
ρ Density of the fluid
σ Electrical conductivity
σ^* Stefan–Boltzmann
τ Skin friction
θ Dimensionless temperature
φ Stream function

Subscript

∞ Ambient condition
w Condition of the wall

1 Introduction

Spectral methods are developing very fast for solving ordinary and partial differential equations [1–4]. Their superior rate of convergence for sufficiently smooth functions seems to be their main appeal. One of the most popular methods of classical spectral category is Tau method which is an approximation technique introduced by Lanczos [5] and used to solve differential equations. The main idea of this approach is implementing a set of orthogonal functions for expanding a function that obtains an approximate solution without demanding to satisfy the boundary conditions by the expansion functions [6–9].

Many problems in science and engineering can be modelled by partial/ordinary differential equations in unbounded/semi-infinite/finite domains, and spectral methods are a promising tool for solving such problems. One direct approach for numerical simulation is using the orthogonal polynomials over unbounded domains, by spectral methods [10–13]. For instance, the Laguerre and Hermite polynomials can be considered in this category. Other approaches like Chebyshev and Jacobi polynomials can be used in bounded domains, but for implementing them, a preprocessing is need that can be satisfied by mapping the original problem in infinite domain to a finite domain [14, 15]. Moreover, the domain truncation method can be used which in, the infinite intervals are replaced by sufficiently large intervals [16]. Using the technique based on the rational approximations is another approach that introduced for the first time by Christov [17] and Boyd [18, 19]. The rational Chebyshev functions defined in [18] and afterward Guo et al. [20] applied the rational Legendre functions as a new set of functions in a spectral method. These two functions are mutually orthogonal on the semi-infinite domain. Therefore, subsequent research was shifted towards solving the nonlinear ordinary differential equations on semi-infinite intervals by applying these rational functions in spectral methods such as collocation and Tau approach based on operational matrix [21–30].

In this paper, we focus on one of the most important orthogonal polynomials, namely Gegenbauer polynomials which are a general case of Chebyshev and Legendre polynomials and make rational Gegenbauer and exponential Gegenbauer functions for solving the systems of nonlinear ordinary differential equations (ODEs) Navier–Stokes equations for micropolar fluids, on a semi-infinite domain. Indeed, the superiority of the rational and exponential Gegenbauer functions for satisfying the boundary conditions defined on a semi-infinite domain than the polynomials basis, appears in solving this type of fluid problem. We use Tau method to solve this problem and present the operational matrices of derivative and product of rational and exponential functions to reduce the solution of this problem to the solution of a system of nonlinear algebraic equations. Also, we analyze the error of function approximation of the method by these types of basis functions which deduces that approximation of the function defined in $[0, \infty)$ is exponential convergence.

In recent years, researchers have become more interested in micropolar fluids flow (a subclass of microfluids) because they are widely used in many applications in industry and science [31, 32]. The theory of micropolar fluids was first introduced by Eringen [33, 34]. This theory demonstrates the effects of local rotary inertia and coupled stresses. Also, it can describe flow behaviour, while classical Newtonian fluid theory is not enough. Łukaszewicz [35] gave comprehensive reviews for both of theory and applications of this research topic in his book. Also, one can refer to [36] for more detail of applications of the micropolar fluids.

The surfaces which in polymer sheets or filaments continuously drawn from a die are denoted by continuous surfaces. The concept of continuous surfaces been proposed by Sakiadis [37]. The boundary layer flow on continuous surfaces is one of the important flow and it appear in some technical operations. Soundalgekar and Takhar investigated the flow and heat transfer past a continuously moving flat plate in a micropolar fluid [38].

With the emergence of the problem of stretching sheet in engineering, Crane [39] was the first researcher who studied the flow generated due to an elastic sheet ant the velocity of it is changed linearly according to the distance that measured from a fixed point on the surface.

Afterwards, subsequent researchers interested in research on stretching sheet and obtained some good results [40, 41]. Chamkha et al. [42] investigated the effects of chemical reaction on unsteady free convective heat and mass transfer on a stretching surface in a porous medium. Ress and Bassom [43] studied the Blasius boundary-layer flow of a micropolar fluid over a flat plate. The subject of heat and mass transfer on a stretching sheet with suction or injection was studied well in [44]. The numerical and approximation methods were investigated for the problem of micropolar fluid from a non-isothermal stretching sheet by considering the concepts of suction and injection in [45] and [46], respectively. Also, the presence of radiation was considered in [47, 48] and they investigated the heat transfer of a micropolar and the flow of a micropolar fluid past a continuously moving, respectively. Damseh et al. [32] considered the problem of combined heat and mass transfer by natural convection of a micropolar, viscous and heat generating or absorbing fluid flow near a continuously moving vertical permeable infinitely long surface in the presence of a first-order chemical reaction. Numerical and analytical solutions of the developing laminar free convection of a micropolar fluid in a vertical parallel plate channel with asymmetric heating were studied in [49]. Rahman et al. [50] studied the two-dimensional steady boundary layer equations for hydro-magnetic convective heat transfer flow of micropolar fluid flowing along a heated inclined flat plate with variable electric conductivity and uniform surface heat flux in the presence of non-uniform heat source or sink. Moreover, in some research, the dependence and influence of another and different parameters on micropolar fluid have been studied [31, 51].

Magnetohydrodynamic (MHD) flows also arise in many applications and several researchers reported studies on MHD-free convection and mass transfer flows [52, 53]. Takhar et al. [54] presented analysis deals with the unsteady flow and heat transfer over a semi-infinite flat plate with an aligned magnetic field and considered plate is impulsively moved with a constant velocity. The presence of heat generation or absorption, and suction or injection effects on steady natural convection boundary-layer flow of a nanofluid was considered in [55]. Seddeek [56] considered the flow of a magneto-micropolar fluid past a continuously moving plate and studied the effect of radiation on the flow of this fluid with suction and blowing in [57]. Moreover, in [58], the MHD micropolar fluid past a stretched permeable surface with heat generation or absorption was studied. Joule heating, chemical reaction and radiation effects on a MHD micropolar fluid were also considered in [59]. Bhargava et al. [60] studied a two-dimensional fully developed steady-state, viscous hydrodynamic flow of a deoxygenated biomagnetic micropolar fluid by finite element method. Recently, Aslani et al. [61] considered the micromagnetorotation (MMR) effect in micropolar MHD flows, by assuming that magnetization and magnetic field vectors are parallel which is applicable in industrial and bioengineering.

Sometimes, the governing nonlinear equations that describe these problems do not have the exact solutions and the solution that comes to mind is using numerical to solve these nonlinear equations [62, 63]. So, the objective of this paper is to investigate the numerical method for equations about the flow of magneto-micropolar fluid by considering radiation and study the effect of different parameters on some important flow characteristics.

The paper continues as follows: In the next section, the set of equations for the problem that is derived from mathematical relationships is described. Sections 3 and 4 review some favourable properties of the rational Gegenbauer functions and exponential Gegenbauer functions, respectively. The convergence rate of these functions approximation is discussed in Sect. 5. In Sect. 6, we use each of these two functions as basis functions in Tau method to solve a system of nonlinear ODEs on the semi-infinite interval and present some numerical results which ensure the accuracy of our method in Sect. 7. Section 8 concludes the paper with a brief summary.

2 Formulation of the problem

The steady, laminar, incompressible, viscous, micropolar and electrically conducting fluid flowing past a continuously moving plate with a constant velocity is assumed [57]. Here, we assumed there is no electric field and the Hall effect of magnetohydrodynamics is neglected. According to [57], the governing equations within boundary layer approximation can be written as

$$\begin{aligned}
&\frac{\partial u}{\partial x}+\frac{\partial v}{\partial y}=0,\\
&u\frac{\partial u}{\partial x}+v\frac{\partial u}{\partial y}=\nu\frac{\partial^2 u}{\partial y^2}+k_1\frac{\partial N}{\partial y}-\frac{\sigma {B_0}^2}{\rho_\infty}u,\\
&G_1\frac{\partial^2 N}{\partial^2 y}-2N-\frac{\partial u}{\partial y}=0,\\
&u\frac{\partial T}{\partial x}+v\frac{\partial T}{\partial y}=\frac{\kappa}{\rho c_p}\frac{\partial^2 T}{\partial y^2}-\frac{1}{\rho c_p}\frac{\partial q_r}{\partial y}+\frac{\nu}{c_p}\left(\frac{\partial u}{\partial y}\right)^2,
\end{aligned} \tag{1}$$

with below boundary conditions

$$\begin{aligned}
&u=bx,\quad v=v_w,\quad N=0,\quad T=T_w,\quad \text{at}\quad y=0,\\
&u\to 0,\quad N\to 0,\quad T\to T_\infty,\quad \text{at}\quad y\to\infty.
\end{aligned} \tag{2}$$

Here u and v are the velocity components along the flow direction (x-direction) and normal to flow direction (y-direction), ν is the kinematic viscosity, N is the components

of microrotation or angular velocity, σ is the electrical conductivity and B_0 is a uniform strong magnetic field in the y-direction. In addition, $k_1 = \frac{s}{\rho}$ is the coupling constant that s is a constant characteristic of the fluid and ρ is the density. G_1 is the microrotation constant, T is the fluid temperature, κ is the thermal conductivity, c_p is the specific heat of the fluid at a constant pressure and q_r is the radiative heat flux.

In boundary conditions, T_w is a constant temperature of the wall, T_∞ is a constant temperature of ambient fluid ($T_\infty > T_w$) and b is constant.

By the Rosseland approximation [64], the radiative heat flux is written as

$$q_r = -\frac{4\sigma^*}{3k^*}\frac{\partial T^4}{\partial y}, \tag{3}$$

where σ^* and k^* are the Stefan-Boltzmann constant and the mean absorption coefficient, respectively. By assumption that the temperature differs in the flow, can expand the term T^4 in a Taylor series about T_∞ and by overlooking the higher-order parts, we have

$$T^4 \simeq 4T_\infty^3 T - 3T_\infty^4. \tag{4}$$

Now, under consideration of the following similarity variables, the governing partial differential equations can convert to a system of coupled nonlinear ordinary differential equation (ODEs)

$$\begin{aligned} &\eta = b^{1/2}v^{-1/2}y, && \varphi = (bv)^{1/2}xf(\eta),\\ &N = b^{3/2}v^{-1/2}xg(\eta), && \theta(\eta) = \frac{T - T_\infty}{T_w - T_\infty}, \end{aligned} \tag{5}$$

where $\varphi(x, y)$ is a stream function such that $u = \frac{\partial \varphi}{\partial y}$ and $v = -\frac{\partial \varphi}{\partial x}$.

So, from the above equations, the transformed equations as systems of nonlinear ordinary differential equation are [57]:

$$\begin{aligned} &f''' + ff'' - (f')^2 - Mf' + Kg' = 0,\\ &Gg'' - (2g + f'') = 0,\\ &\left(\frac{1+R}{R\mathrm{Pr}}\right)\theta'' + f\theta' - \gamma f'\theta + \mathrm{Ec}(f'')^2 = 0, \end{aligned} \tag{6}$$

and the boundary conditions on a semi-infinite computational domain as follow:

$$\begin{aligned} &f(0) = f_w, \quad f'(0) = 1, \quad f'(\infty) = 0,\\ &g(0) = 0, \quad g(\infty) = 0,\\ &\theta(0) = 1, \quad \theta(\infty) = 0, \end{aligned} \tag{7}$$

where f, g and θ are similarity functions for velocity, microrotation and temperature, respectively and their derivatives are respect to η (similarity variables), γ is a constant parameter. The important physical parameters are as follow:

$$\begin{aligned} &\mathrm{Pr} = \frac{\rho c_p v}{K}, && M = \frac{\sigma {B_0}^2}{\rho_\infty B},\\ &R = \frac{3Kk^*}{16\sigma^* {T_\infty}^3}, && K = \frac{k_1}{v},\\ &G = \frac{G_1 B}{v}, && \mathrm{Ec} = \frac{{u_w}^2}{c_p(T_w - T_\infty)}, \end{aligned} \tag{8}$$

that they are the Prandtl number, magnetic field parameter, radiation parameter, coupling constant parameter, microrotation number and Eckert number, respectively.

For the suction and injection case f_w is positive, negative, respectively. The skin friction of the considered surface can be obtained as [45]:

$$\tau_w = -\mu_w (u_w)^{3/2}(vx)^{-1/2} f''(0). \tag{9}$$

With considering $Re = \frac{u_w x}{v}$ as the Reynolds number, the friction coefficient (c_f), heat flux (q_w) and Nusselt number (Nu) are as follow:

$$\begin{aligned} &c_f = -(Re)^{-1/2} f''(0)\\ &q_w = -K(T_w - T_\infty)(u_w)^{1/2}(vx)^{-1/2}\theta'(0),\\ &\mathrm{Nu} = -(Re)^{1/2}\theta'(0). \end{aligned} \tag{10}$$

3 Rational Gegenbauer functions

In this section, the definition of rational Gegenbauer functions and their properties will be presented. Let n be an integer variable, the Gegenbauer polynomials of degree n are defined as follow [65]:

$$G_n^\alpha(t) = \sum_{j=0}^{[n/2]} (-1)^j \frac{\Gamma(n + \alpha - j)}{j!(n-2j)!\Gamma(\alpha)}(2t)^{n-2j} \quad \text{for } \alpha > -\frac{1}{2}, \tag{11}$$

where Γ is the Gamma function.

These polynomials are orthogonal in $[-1, 1]$, with the following weight function $\rho(t) = (1 - t^2)^{\alpha - \frac{1}{2}}$, for a fixed value of α, G_n^α can be obtained as [66]:

$$\begin{cases} G_0^\alpha(t) = 1,\\ G_1^\alpha(t) = 2\alpha t,\\ G_{n+1}^\alpha(t) = \frac{1}{n+1}\left[2y(n+\alpha)G_n^\alpha(t) - (n + 2\alpha - 1)G_{n-1}^\alpha(t)\right], \quad n \geq 1. \end{cases} \tag{12}$$

With considering the new basis functions according to the Gegenbauer polynomials and call them rational

Gegenbauer functions as $R_n^{\alpha}(x)=G_n^{\alpha}(\frac{x-L}{x+L})$, where $\alpha>-\frac{1}{2}$ and L is a constant parameter, which one can properly choose it to adjusts the length of the desired interval [67]. The following recursive formulas for $R_n^{\alpha}(x)$ can be derived easily:

$$\begin{cases} R_0^{\alpha}(x)=1, \\ R_1^{\alpha}(x)=2\alpha\dfrac{x-L}{x+L}, \\ R_{n+1}^{\alpha}(x)=\dfrac{1}{n+1}\left[2\left(\dfrac{x-L}{x+L}\right)(n+\alpha)R_n^{\alpha}(x)-(n+2\alpha-1)R_{n-1}^{\alpha}(x)\right], n\geq 1. \end{cases} \tag{13}$$

It should be mentioned that the weight function is: $w_r^{\alpha}(x)=\frac{2L}{(x+L)^2}\left[1-\left(\frac{x-L}{x+L}\right)^2\right]^{\alpha-\frac{1}{2}}$, and the orthogonality the interval is a semi-infinite domain as: $[0,\infty)$. The following integral formula can be considered for the orthogonal functions:

$$\int_0^{\infty} R_n^{\alpha}(x)R_m^{\alpha}(x)w_r^{\alpha}(x)\mathrm{d}x=\frac{\pi 2^{1-2\alpha}\Gamma(n+2\alpha)}{n!(n+\alpha)\Gamma^2(\alpha)}\delta_{nm}, \tag{14}$$

where δ_{nm} is the Kronecker function. The differentiation formula for Gegenbauer polynomials is [65]:

$$\dot{G}_n^{\alpha}(t)=\frac{d}{dt}G_n^{\alpha}(t)=2\alpha G_{n-1}^{\alpha+1}(t), \tag{15}$$

therefore, the following formula for the derivative can be obtained:

$$\dot{R}_n^{\alpha}(x)=\frac{\mathrm{d}}{\mathrm{d}x}R_n^{\alpha}(x)=\frac{4\alpha L}{(x+L)^2}R_{n-1}^{\alpha+1}(x). \tag{16}$$

With respect to Eqs. (14) and (16), we discover that $\dot{R}_n^{\alpha}(x)$ are also mutually orthogonal considering the weight function $\widehat{w_{\mathrm{r}}^{\alpha}}(x)=\frac{(x+L)^2}{8L\alpha^2}\left[1-\left(\frac{x-L}{x+L}\right)^2\right]^{\alpha+\frac{1}{2}}$. Hence

$$\int_0^{\infty}\dot{R}_n^{\alpha}(x)\dot{R}_n^{\alpha}(x)\widehat{w_{\mathrm{r}}^{\alpha}}(x)\mathrm{d}x=\frac{\pi 2^{-(2\alpha+1)}\Gamma(2\alpha+n+1)}{(n-1)!(n+\alpha)\Gamma^2(\alpha+1)}\delta_{nm}. \tag{17}$$

Function approximation An arbitrary function $\varphi(x)$ on the semi-infinite interval $[0,\infty)$ can be expanded with a fixed value of α as:

$$\varphi(x)=\sum_{j=0}^{\infty}a_jR_j^{\alpha}(x), \tag{18}$$

where

$$a_j=\frac{j!(j+\alpha)\Gamma^2(\alpha)}{\pi 2^{1-2\alpha}\Gamma(j+2\alpha)}\int_0^{\infty}R_j^{\alpha}(x)\varphi(x)w_{\mathrm{r}}^{\alpha}(x)\mathrm{d}x. \tag{19}$$

If $\varphi(x)$ in Eq. (18) is truncated after the Nth terms, then

$$\varphi_N(x)=\sum_{j=0}^{N-1}a_jR_j^{\alpha}(x)=A^TR^{\alpha}(x), \tag{20}$$

where the entity of A and $R^{\alpha}(x)$ vectors are listed as unknown coefficients and rational Gegenbauer functions with different degrees:

$$A=[a_0,a_1,...,a_{N-1}]^{\mathrm{T}}, \tag{21}$$

$$R^{\alpha}(x)=[R_0^{\alpha}(x),R_1^{\alpha}(x),...,R_{N-1}^{\alpha}(x)]^{\mathrm{T}}. \tag{22}$$

Derivative operational matrix The derivative of the vector $R^{\alpha}(x)$ [Eq. (22)], is a matrix:

$$\dot{R}^{\alpha}(x)=\frac{\mathrm{d}R^{\alpha}(x)}{\mathrm{d}x}\simeq D_rR^{\alpha}(x). \tag{23}$$

For obtaining the elements of square matrix $(N\times N)$, the following recursive formula can be implemented:

$$\begin{cases} \dot{R}_0^{\alpha}(x)=0, \\ \dot{R}_1^{\alpha}(x)=\dfrac{4\alpha L}{(x+L)^2}=\dfrac{1}{L}\left[\dfrac{\alpha(3+2\alpha)}{2(\alpha+1)}R_0^{\alpha}(x)-R_1^{\alpha}(x)+\dfrac{1}{2(\alpha+1)}R_2^{\alpha}(x)\right], \\ \dot{R}_{n+1}^{\alpha}(x)=\dfrac{1}{n+1}\left[(\dfrac{n}{\alpha}+1)\dfrac{\mathrm{d}}{\mathrm{d}x}(R_n^{\alpha}(x)\cdot R_1^{\alpha}(x))-(n+2\alpha-1)\dot{R}_{n-1}^{\alpha}(x)\right], n\geq 1. \end{cases} \tag{24}$$

Therefore one can figure out that D_r, is a lower-Hessenberg matrix and can be defined as $D_r=\frac{D_1+D_2}{L}$; where D_1 can be formulated by considering all elements of the first row $(i=0)$ are zero and other elements obtained from the following tridiagonal matrix

$$\begin{aligned} D_1=&\mathrm{diag}\left(\frac{\alpha^2}{\alpha+i}+\frac{3(2i-1)\alpha}{2(\alpha+i)}+\frac{7i(i-1)}{4(\alpha+i)},\right. \\ &\left.-i,\frac{i(i+1)}{4(\alpha+i)}\right), i=1,\ldots,N-1, \end{aligned} \tag{25}$$

and the entities of matrix D_2 are determined by $d_{10}=\frac{3}{2}$ if $\alpha=0$ and the following conditional expression for other elements

$$d_{ij}=\begin{cases} 0, & j\geq i-1, \\ (-1)^{i+j+1}c_{\alpha j}, & j<i-1, \end{cases} \tag{26}$$

where $c_{00}=2$ and $c_{\alpha j}=2(\alpha+j)$ for other cases.

According to the previous formula, for a fixed value of $\alpha\neq 0$ and considering $N=5$, the derivative operational matrix will have the following form:

$$D_r = \frac{1}{L}\begin{pmatrix} 0 & 0 & 0 & 0 & 0 \\ \frac{\alpha(2\alpha+3)}{2(\alpha+1)} & -1 & \frac{1}{2(\alpha+1)} & 0 & 0 \\ -2\alpha & \frac{(\alpha+1)(2\alpha+7)}{2(\alpha+2)} & -2 & \frac{3}{2(\alpha+2)} & 0 \\ 2\alpha & -2(\alpha+1) & \frac{2\alpha^2+15\alpha+21}{2(\alpha+3)} & -3 & \frac{3}{\alpha+3} \\ -2\alpha & 2(\alpha+1) & -2(\alpha+2) & \frac{2\alpha^2+21\alpha+42}{2(\alpha+4)} & -4 \end{pmatrix}.$$

Moreover, if we consider $\alpha = 0$ and $L = 1$, the matrix is as follows

$$D_r = \begin{pmatrix} 0 & 0 & 0 & 0 & 0 \\ 3/2 & -1 & 1/2 & 0 & 0 \\ -2 & 7/4 & -2 & 3/4 & 0 \\ 2 & -3 & 7/2 & -3 & 1 \\ -2 & 3 & -5 & 21/4 & -4 \end{pmatrix}.$$

Product operational matrix In producting the two rational Gegenbauer function vectors we have the following property:

$$R^{\alpha}(x)[R^{\alpha}]^{\mathrm{T}}(x)A \simeq \tilde{A}R^{\alpha}(x), \tag{27}$$

in which $\tilde{A}$ is an $N \times N$ product operational matrix for the vector A whose elements can be calculated from the below equation by upper property and the orthogonal property Eq. (14):

$$\tilde{a}_{ij} = \frac{j!(j+\alpha)\Gamma^2(\alpha)}{\pi 2^{1-2\alpha}\Gamma(j+2\alpha)}\sum_{k=0}^{N-1} a_k \int_0^{\infty} R_i^{\alpha}(x)R_j^{\alpha}(x)R_k^{\alpha}(x)w_r^{\alpha}(x)\mathrm{d}x. \tag{28}$$

4 Exponential Gegenbauer functions

We now pay our attention to the exponential Gegenbauer functions which are orthogonal functions on the semi-infinite domain and we introduce them for the first time. The exponential Gegenbauer (E) functions can be defined by $E_n^{\alpha}(x) = G_n^{\alpha}(1-2e^{-\frac{x}{L}})$, where $\alpha > -\frac{1}{2}$ and the desired interval length is adjusted by parameter L. The recursive formula for these functions are:

$$\begin{cases} E_0^{\alpha}(x) = 1, \\ E_1^{\alpha}(x) = 2\alpha(1-2e^{-\frac{x}{L}}), \\ E_{n+1}^{\alpha}(x) = \frac{1}{n+1}\left[2(1-2e^{-\frac{x}{L}})(n+\alpha)E_n^{\alpha}(x) - (n+2\alpha-1)E_{n-1}^{\alpha}(x)\right], n \geq 1. \end{cases} \tag{29}$$

Exponential Gegenbauer functions are also orthogonal on the semi-infinite domain with respect to weighting function $w_e^{\alpha}(x) = \frac{2}{L}e^{-\frac{x}{L}}\left[4e^{-\frac{x}{L}}(1-e^{-\frac{x}{L}})\right]^{\alpha-\frac{1}{2}}$ and the orthogonality integral equation, similar to Eq. (14) is as follows:

$$\int_0^{\infty} E_n^{\alpha}(x)E_m^{\alpha}(x)w_e^{\alpha}(x)\mathrm{d}x = \frac{\pi 2^{1-2\alpha}\Gamma(n+2\alpha)}{n!(n+\alpha)\Gamma^2(\alpha)}\delta_{nm}, \tag{30}$$

The derivative of the exponential Gegenbauer functions is:

$$\dot{E}_n^{\alpha}(x) = \frac{\mathrm{d}}{\mathrm{d}x}E_n^{\alpha}(x) = \frac{4\alpha}{L}e^{-\frac{x}{L}}E_{n-1}^{\alpha+1}(x). \tag{31}$$

If consider $\widehat{w_e^{\alpha}}(x) = \frac{L}{8\alpha^2}e^{-\frac{x}{L}}\left[4e^{-\frac{x}{L}}(1-e^{-\frac{x}{L}})\right]^{\alpha+\frac{1}{2}}$ as the weight function of $\dot{E}_n^{\alpha}(x)$'s functions, then the same quotation in Eq. (17) for the orthogonality property of these functions will be obtained.

Function approximation As mentioned before, to approximate a function on a semi-infinite domain, one can use Eq. (18). In this research, $E_j^{\alpha}(x)$ is used as basis functions instead of $R_j^{\alpha}(x)$:

$$\varphi(x) = \sum_{j=0}^{\infty} a_j E_j^{\alpha}(x), \tag{32}$$

that

$$a_j = \frac{j!(j+\alpha)\Gamma^2(\alpha)}{\pi 2^{1-2\alpha}\Gamma(j+2\alpha)}\int_0^{\infty} E_j^{\alpha}(x)\varphi(x)w_e^{\alpha}(x)\mathrm{d}x. \tag{33}$$

Therefore:

$$\varphi_N(x) = \sum_{j=0}^{N-1} a_j E_j^{\alpha}(x) = A^T E^{\alpha}(x), \tag{34}$$

it should be mentioned that the entity of A and $E^{\alpha}(x)$ vectors are unknown coefficient and exponential Gegenbauer functions with different degrees, respectively:

$$A = [a_0, a_1, ..., a_{N-1}]^{\mathrm{T}}, \tag{35}$$

$$E^{\alpha}(x) = [E_0^{\alpha}(x), E_1^{\alpha}(x), ..., E_{N-1}^{\alpha}(x)]^{\mathrm{T}}. \tag{36}$$

Derivative operational matrix By using a $N \times N$ derivative matrix (D_e) which will be defined later, the following formula for the derivative of the vector $E^{\alpha}(x)$ will be obtained:

$$\dot{E}^{\alpha}(x) = \frac{dE^{\alpha}(x)}{\mathrm{d}x} \simeq D_e E^{\alpha}(x). \tag{37}$$

By deriving each of the expressions in Eq. (29):

$$\begin{cases} \dot{E}_0^{\alpha}(x) = 0. \\ \dot{E}_1^{\alpha}(x) = \dfrac{4\alpha}{L} e^{-\frac{x}{L}} = \dfrac{1}{L}\left[2\alpha E_0^{\alpha}(x) - E_1^{\alpha}(x)\right], \\ \dot{E}_{n+1}^{\alpha}(x) = \dfrac{1}{n+1}\left[(\dfrac{n}{\alpha}+1)\dfrac{\mathrm{d}}{\mathrm{d}x}(E_n^{\alpha}(x)\cdot E_1^{\alpha}(x)) - (n+2\alpha-1)\dot{E}_{n-1}^{\alpha}(x)\right], n \geq 1. \end{cases} \tag{38}$$

Based on the above equations, a low-triangular matrix is obtained, and $D_e = \frac{\overline{D}_1 + \overline{D}_2}{L}$; where $\overline{D}_1$ is a diagonal matrix and defined as $D_1 = \mathrm{diag}\,(-i)$ for $i = 0, \ldots, N-1$ and $\overline{D}_2$ is defined as follow

$$d_{ij} = \begin{cases} 0, & j > i-1, \\ (-1)^{i+j+1} c_{\alpha j}, & j \leq i-1, \end{cases} \tag{39}$$

where $c_{00} = 2$ and otherwise $c_{\alpha j} = 2(\alpha + j)$.

For $N = 5$ and fixed $\alpha \neq 0$ the final matrix will be obtained:

$$D_e = \frac{1}{L}\begin{pmatrix} 0 & 0 & 0 & 0 & 0 \\ 2\alpha & -1 & 0 & 0 & 0 \\ -2\alpha & 2(\alpha+1) & -2 & 0 & 0 \\ 2\alpha & -2(\alpha+1) & 2(\alpha+2) & -3 & 0 \\ -2\alpha & 2(\alpha+1) & -2(\alpha+2) & 2(\alpha+3) & -4 \end{pmatrix}.$$

Also, if we consider $\alpha = 0$ and $L = 1$, the matrix is as follows

$$D_e = \begin{pmatrix} 0 & 0 & 0 & 0 & 0 \\ 2 & -1 & 0 & 0 & 0 \\ -2 & 2 & -2 & 0 & 0 \\ 2 & -2 & 4 & -3 & 0 \\ -2 & 2 & -4 & 6 & -4 \end{pmatrix}.$$

As it can be seen, the form of this matrix is simpler than that of the derivation matrix for $R^{\alpha}(x)$. Consequently, It can be computed faster. In addition, D_e is a lower-triangular matrix but D_r is a lower-Hessenberg matrix, so there exists more zero elements in D_e.

Product operational matrix With considering the production of two exponential Gegenbauer function vectors over a vector A, a matrix $\tilde{A}$ as below:

$$E^{\alpha}(x)[E^{\alpha}]^{\mathrm{T}}(x)A \simeq \tilde{A}E^{\alpha}(x), \tag{40}$$

The entities $\tilde{a}_{ij}$ of the matrix $\tilde{A}$ can be calculated similar to Eq. (28) except applying exponential functions and related weights instead of the rational functions and their associated weights:

$$\tilde{a}_{ij} = \frac{j!(j+\alpha)\Gamma^2(\alpha)}{\pi 2^{1-2\alpha}\Gamma(j+2\alpha)} \sum_{k=0}^{N-1} a_k \int_0^{\infty} E_i^{\alpha}(x) E_j^{\alpha}(x) E_k^{\alpha}(x) w_e^{\alpha}(x)\mathrm{d}x. \tag{41}$$

5 Convergence of the function approximation

In this section an error bound of both rational and exponential Gegenbauer functions approximation are estimated and we show that by increasing N, the approximation solution $\varphi_N(x)$ [Eqs. (20) and (34)] is convergent to $\varphi(x)$ [Eqs. (18) and (32)] exponentially.

Let consider the fixed α and $w(x)$ be $w_{\mathrm{r}}^{\alpha}(x)$ or $w_e^{\alpha}(x)$ which are nonnegative, integrable and real-valued weight functions over the interval $I = [0, \infty)$.

Here, we define

$$L_w^2(I) = \{v : I \to \mathbb{R} \mid v \text{ is measurable and } \| v \|_w < \infty\}, \tag{42}$$

where

$$\| v \|_w = (\int_0^{\infty} v^2(x) w(x)\mathrm{d}x)^{\frac{1}{2}}, \tag{43}$$

is the norm induced by the scalar product

$$\langle u, v \rangle_w = \int_0^{\infty} u(x) v(x) w(x)\mathrm{d}x. \tag{44}$$

Thus, $\{\psi_j(x)\}_{j\geq 0}$ as $\{R_j^{\alpha}(x)\}_{j\geq 0}$ or $\{E_j^{\alpha}(x)\}_{j\geq 0}$ denotes a system which is mutually orthogonal with respect to its weight function w as w_{r}^{α} or w_e^{α} under Eq. (44), i.e.

$$\langle \psi_n, \psi_m \rangle_{\mathrm{w}} = \frac{\pi 2^{1-2\alpha}\Gamma(n+2\alpha)}{n!(n+\alpha)\Gamma^2(\alpha)} \delta_{nm}, \tag{45}$$

and is complete in the space $L_w^2(I)$.

Now, if consider one of the equations of (20) and (34) for approximation of any function $\varphi(x) \in L_w^2(I)$ we can determine the following error:

$$e_N = \| \varphi(x) - \varphi_N(x) \|_{\mathrm{w}}^2 . \tag{46}$$

By the completeness of the system $\{\psi_j(x)\}_{j\geq 0}$, when $N \to \infty$, we have $\varphi_N(x) \to \varphi(x)$ and $e_N \to 0$. Furthermore this completeness and definition of $\| \ . \ \|_{\mathrm{w}}$ release to rewrite the error in Eq. (46) as

$$\begin{aligned} e_N &= \| \sum_{i=N}^{\infty} a_i \psi_i(x) \|_{\mathrm{w}}^2 = \sum_{i=N}^{\infty} \sum_{j=N}^{\infty} a_i a_j \langle \psi_i(x), \psi_j(x) \rangle_{\mathrm{w}} \\ &= \sum_{i=N}^{\infty} \sum_{j=N}^{\infty} a_i a_j \frac{\pi 2^{1-2\alpha} \Gamma(i+2\alpha)}{i!(i+\alpha)\Gamma^2(\alpha)} \delta_{ij} \\ &= \sum_{i=N}^{\infty} \frac{\pi 2^{1-2\alpha} \Gamma(i+2\alpha) a_i^2}{i!(i+\alpha)\Gamma^2(\alpha)}, \end{aligned} \tag{47}$$

and according to Eqs. (19) and (33) we have

$$e_N = \sum_{i=N}^{\infty} \frac{i!(i+\alpha)\Gamma^2(\alpha)}{\pi 2^{1-2\alpha}\Gamma(i+2\alpha)} \langle \varphi(x), \psi_i(x) \rangle_{\mathrm{w}}^2. \tag{48}$$

This equation shows that the convergence rate is involved with function $\varphi(x)$. Now, since $\varphi(x) \in L_w^2(I)$, we could present the following theorem about an upper bound for estimating the error of function approximation by $\psi_i(x)$. One Gegenbauer polynomials property which can be helped our proof of the theorem is [68]:

$$x^n = \sum_{0\leq k\leq n, n-k\equiv 0 \pmod 2} \frac{(k+\alpha)n!\Gamma(\alpha)}{2^n (\frac{n-k}{2})! \Gamma(\frac{n+k+2\alpha+2}{2})} G_k^{\alpha}(x). \tag{49}$$

Theorem 1 *Suppose that $\varphi_N(x)$ which is obtained by Eq. (20) or (34) is the best approximation to $\varphi(x) \in L_{\mathrm{w}}^2(I)$ and $\mathcal{F}(y) = \varphi(\Phi(y))$ is analytic on $[-1, 1]$, then an error bound is presented as follows:*

$$e_N \leq \sum_{i=N}^{\infty} \frac{\pi 2^{1-2i-2\alpha}\Gamma(i+2\alpha) M_i^2}{(i+\alpha)\Gamma^2(i+\alpha)\Gamma(i+1)} \tag{50}$$

where $\Phi(y) = L\left(\frac{1+y}{1-y}\right)$ or $-L\ln\left(\frac{1-y}{2}\right)$ *and* $M_i = \max |\mathcal{F}^{(i)}(y)|, y \in (-1, 1)$.

Proof For two cases of $\Phi(y)$ as rational and exponential mapping, we have the following properties:

Rational mapping

$$: \begin{cases} \Phi(y) = L\left(\dfrac{1+y}{1-y}\right), \quad R_n^{\alpha}(\Phi(y)) = G_n^{\alpha}(y), \\ w_{\mathrm{r}}^{\alpha}(\Phi(y)) = \dfrac{(1-y)^2}{2L}(1-y^2)^{\alpha-\frac{1}{2}}, \quad \mathrm{d}x = \dfrac{2L}{(1-y)^2}\mathrm{d}y. \end{cases}$$

Exponential mapping

$$: \begin{cases} \Phi(y) = -L\ln\left(\dfrac{1-y}{2}\right), \quad E_n^{\alpha}(\Phi(y)) = G_n^{\alpha}(y), \\ w_e^{\alpha}(\Phi(y)) = \dfrac{1-y}{L}(1-y^2)^{\alpha-\frac{1}{2}}, \quad \mathrm{d}x = \dfrac{L}{1-y}\mathrm{d}y. \end{cases}$$

Now, if consider each case in $\langle \varphi(x), \psi_i(x) \rangle_{\mathrm{w}}$ we have:

$$\langle \varphi(x), \psi_i(x) \rangle_{\mathrm{w}} = \int_{-1}^{1} \mathcal{F}(y) G_i^{\alpha}(y) w(y) \mathrm{d}y. \tag{51}$$

Since $\mathcal{F}(y)$ is analytical, can have the Taylor's formula for $i \geq N$ as follow:

$$\begin{aligned} \langle \varphi(x), \psi_i(x) \rangle_{\mathrm{w}} &= \sum_{h=0}^{i-1} \frac{\mathcal{F}^{(h)}(0)}{h!} \int_{-1}^{1} y^h G_i^{\alpha}(y) w(y) \mathrm{d}y \\ &+ \frac{\mathcal{F}^{(i)}(\xi_i)}{i!} \int_{-1}^{1} y^i G_i^{\alpha}(y) w(y) \mathrm{d}y, \quad \xi_i \in (-1, 1). \end{aligned}$$

According to Eq. (49) and because of the orthogonality of the basis functions,

$$\int_{-1}^{1} y^h G_i^{\alpha}(y) w(y) \mathrm{d}y = 0, \quad h = 0, 1, \ldots, i-1, \tag{52}$$

and the remaining phrase respect to Eq. (49), can be rewritten as the following:

$$\begin{aligned} &\langle \varphi(x), \psi_i(x) \rangle_{\mathrm{w}} \\ &= \frac{\mathcal{F}^{(i)}(\xi_i)}{i!} \frac{\pi i! 2^{1-2\alpha}\Gamma(i+2\alpha)}{i! 2^i \Gamma(\alpha)\Gamma(i+1+\alpha)} \\ &\leq \frac{\pi 2^{1-2\alpha}\Gamma(i+2\alpha) M_i}{i! 2^i \Gamma(\alpha)\Gamma(i+1+\alpha)}. \end{aligned} \tag{53}$$

So, by substituting above inequality in Eq. (48), the proof is completed. □

This theorem demonstrates that any function defined in $L_{\mathrm{w}}^2(I)$, which their rational and exponential mapping are analytic, has a series solution in the forms Eqs. (20) and (34), respectively, with the exponential convergence.

6 RGT and EGT method for solving the problem

In this part, the proposed functions in Tau method was implemented to the rational Gegenbaure Tau (RGT) and the exponential Gegenbaure Tau (EGT) methods to solve Eq. (6). After choosing a value for α parameter, and considering $\psi(\eta) = R^{\alpha}(\eta)$ in the following formulas to solve the problem. Then assume $\psi(\eta) = E^{\alpha}(\eta)$ and apply EGT method. For comparison the obtained results are compared with RGT and EGT methods. The three functions in Eq. (6) and their derivatives are as follows:

$$f(\eta) \simeq f_N(\eta), \tag{54}$$

$$f_N(\eta) = \sum_{i=0}^{N-1} a_i \psi_i(\eta) = A^T \psi(\eta), \tag{55}$$

$$f_N^{(j)}(\eta) = \sum_{i=0}^{N-1} a_i \psi_i{}^{(j)}(\eta) \simeq A^T D^j \psi(\eta) \quad j = 1, 2, 3, \tag{56}$$

$$g(\eta) \simeq g_N(\eta), \tag{57}$$

$$g_N(\eta) = \sum_{i=0}^{N-1} b_i \psi_i(\eta) = B^T \psi(\eta), \tag{58}$$

$$g_N^{(j)}(\eta) = \sum_{i=0}^{N-1} b_i \psi_i{}^{(j)}(\eta) \simeq B^T D^j \psi(\eta) \quad j = 1, 2, \tag{59}$$

$$\theta(\eta) \simeq \theta_N(\eta), \tag{60}$$

$$\theta_N(\eta) = \sum_{i=0}^{N-1} c_i \psi_i(\eta) = C^T \psi(\eta), \tag{61}$$

$$\theta_N^{(j)}(\eta) = \sum_{i=0}^{N-1} c_i \psi_i{}^{(j)}(\eta) \simeq C^T D^j \psi(\eta) \quad j = 1, 2, \tag{62}$$

where D^j is obtained by multiplying it by itself j-times and it can be D_r or D_e given in Eqs. (23) or (37). By using above equations, then

$$\begin{aligned} f_N(\eta) f_N''(\eta) &\simeq A^T \psi(\eta) \psi^T(\eta) (D^2)^T A \\ &= A^T \psi(\eta) \psi^T(\eta) U \simeq A^T \tilde{U} \psi(\eta), \end{aligned} \tag{63}$$

$$\begin{aligned} f_N'^2(\eta) &\simeq A^T D \psi(\eta) \psi^T(\eta) D^T A \\ &= A^T D \psi(\eta) \psi^T(\eta) V \simeq A^T D \tilde{V} \psi(\eta), \end{aligned} \tag{64}$$

$$\begin{aligned} f_N''^2(\eta) &\simeq A^T D^2 \psi(\eta) \psi^T(\eta) (D^2)^T A \\ &= A^T D^2 \psi(\eta) \psi^T(\eta) U \simeq A^T D^2 \tilde{U} \psi(\eta), \end{aligned} \tag{65}$$

$$\begin{aligned} f_N(\eta) \theta_N'(\eta) &\simeq A^T \psi(\eta) \psi^T(\eta) D^T C \\ &= A^T \psi(\eta) \psi^T(\eta) W \simeq A^T \tilde{W} \psi(\eta), \end{aligned} \tag{66}$$

$$\begin{aligned} f_N'(\eta) \theta_N(\eta) &\simeq A^T D \psi(\eta) \psi^T(\eta) C \\ &\simeq A^T D \tilde{C} \psi(\eta), \end{aligned} \tag{67}$$

where $U = (D^2)^T A$, $V = D^T A$, $W = D^T C$ and the elements of matrices $\tilde{U}$, $\tilde{V}$, $\tilde{W}$ and $\tilde{C}$, can be calculated similar to Eqs. (28) and (41).

Now, consider the three equation in Eq. (6), the following residual functions $(\mathrm{Res}_1(\eta), \mathrm{Res}_2(\eta), \mathrm{Res}_3(\eta))$ can be considered:

$$\begin{aligned} \mathrm{Res}_1(\eta) = [&A^T D^3 + A^T \tilde{U} - A^T D \tilde{V} - M A^T D \\ &+ K B^T D] \psi(\eta), \end{aligned} \tag{68}$$

$$\mathrm{Res}_2(\eta) = [G B^T D^2 - (2B^T + A^T D^2)] \psi(\eta), \tag{69}$$

$$\begin{aligned} \mathrm{Res}_3(\eta) = \Big[&\left(\frac{1+R}{R\mathrm{Pr}} \right) C^T D^2 + A^T \tilde{W} - \gamma A^T D \tilde{C} \\ &+ \mathrm{Ec}(A^T D^2 \tilde{U}) \Big] \psi(\eta). \end{aligned} \tag{70}$$

Now, by applying the Tau method [1, 6, 22], $3(N-2)$ algebraic equations by the following equations will be obtained:

$$\begin{aligned} &\langle \mathrm{Res}_1(\eta), \psi_k(\eta) \rangle \\ &= \int_0^\infty \mathrm{Res}_1(\eta) \psi_k(\eta) w(\eta) d\eta = 0, \quad k = 0, 1, \ldots N-3, \end{aligned} \tag{71}$$

$$\begin{aligned} &\langle \mathrm{Res}_2(\eta), \psi_k(\eta) \rangle \\ &= \int_0^\infty \mathrm{Res}_2(\eta) \psi_k(\eta) w(\eta) d\eta = 0, \quad k = 0, 1, \ldots N-3, \end{aligned} \tag{72}$$

$$\begin{aligned} &\langle \mathrm{Res}_3(\eta), \psi_k(\eta) \rangle \\ &= \int_0^\infty \mathrm{Res}_3(\eta) \psi_k(\eta) w(\eta) d\eta = 0, \quad k = 0, 1, \ldots N-3, \end{aligned} \tag{73}$$

Note that $w(\eta)$ in the above equations, is the weight function and can be chosen as $w_r^\alpha(\eta)$ or $w_e^\alpha(\eta)$ according to the selected method.

With implementing the boundary conditions:

$$\begin{aligned} &f_N(0) \\ &= A^T \psi(0) = f_w, \quad f_N'(0) = A^T D \psi(0) = 1, \end{aligned} \tag{74}$$

$$\begin{aligned} &g_N(0) \\ &= B^T \psi(0) = 0, \quad \lim_{\eta \to \infty} g_N(\eta) \\ &= \lim_{\eta \to \infty} B^T \psi(\eta) = 0, \end{aligned} \tag{75}$$

$$\begin{aligned} &\theta_N(0) \\ &= C^T \psi(0) = 1, \quad \lim_{\eta \to \infty} \theta_N(\eta) \\ &= \lim_{\eta \to \infty} C^T \psi(\eta) = 0, \end{aligned} \tag{76}$$

and another boundary condition $(f'(\infty) = 0)$ is already satisfied.

Among to Eqs. (71)–(76), a system of nonlinear equations with $3N$ equations and $3N$ unknown coefficients include a_i, b_i and c_i of the vector A, B and C in Eqs. (55), (58) and (61) are obtained which can be calculated.

Table 1 The residual functions for three equations in main problem by using RGT and EGT methods with various α and N, when $M = 2, K = 1, f_w = 0, \Pr = 10, R = 3, \gamma = 1, G = 2$ and $\mathrm{Ec} = 0.02$

α	N	RGT			EGT		
		$\|\|\mathrm{Res}_1\|\|^2$	$\|\|\mathrm{Res}_2\|\|^2$	$\|\|\mathrm{Res}_3\|\|^2$	$\|\|\mathrm{Res}_1\|\|^2$	$\|\|\mathrm{Res}_2\|\|^2$	$\|\|\mathrm{Res}_3\|\|^2$
− 0.4	5	1.82E−02	6.84E−02	6.52E−03	5.57E−02	4.19E−02	6.69E−02
	7	9.59E−03	3.86E−03	1.67E−02	2.38E−06	4.16E−08	2.22E−03
	11	2.38E−04	6.18E−06	4.43E−05	3.08E−11	9.28E−10	6.67E−06
	15	7.71E−08	6.31E−08	2.21E−07	5.71E−14	1.21E−10	8.42E−09
0	5	1.51E−02	6.54E−02	5.49E−03	2.98E−02	2.22E−02	2.83E−02
	7	1.55E−02	4.86E−03	8.03E−03	1.36E−06	4.74E−08	9.14E−04
	11	1.07E−04	6.03E−06	1.48E−05	2.10E−11	5.43E−11	3.27E−06
	15	4.94E−08	1.57E−08	1.45E−07	2.21E−17	8.99E−14	3.94E−09
0.5	5	5.98E−02	1.07E−01	4.13E−03	2.28E−02	1.65E−02	1.66E−02
	7	2.51E−02	7.42E−03	3.55E−03	1.04E−06	5.95E−08	5.26E−04
	11	5.36E−04	1.99E−05	2.55E−05	1.73E−11	6.51E−11	4.25E−06
	15	5.90E−08	5.10E−08	1.87E−07	4.55E−14	9.93E−11	5.19E−09
1.5	5	9.99E−02	1.46E−01	2.32E−03	2.96E−02	1.97E−02	1.37E−02
	7	4.94E−02	1.66E−02	4.12E−03	2.11E−06	1.76E−07	8.53E−04
	11	1.94E−03	9.29E−05	5.13E−05	5.39E−11	4.51E−10	6.50E−06
	15	1.69E−07	5.32E−07	2.01E−07	6.31E−12	7.95E−10	2.03E−08
2.5	5	1.24E−01	1.77E−01	1.50E−03	4.25E−02	2.69E−02	1.62E−02
	7	7.80E−02	3.14E−02	6.65E−03	4.86E−06	5.15E−07	1.39E−03
	11	5.14E−03	2.97E−04	3.27E−04	2.37E−10	1.32E−11	1.82E−05
	15	1.88E−05	4.08E−06	3.49E−06	1.29E−12	7.04E−10	8.14E−08
3.5	5	1.38E−01	2.02E−01	1.20E−03	5.50E−02	3.40E−02	1.93E−02
	7	1.08E−01	5.26E−02	7.91E−03	8.59E−06	1.12E−06	1.70E−03
	11	1.12E−02	7.22E−04	1.08E−03	7.12E−10	7.27E−11	2.30E−05
	15	6.34E−05	1.94E−05	2.35E−05	1.45E−12	3.70E−11	1.59E−07

7 Numerical results and discussions

In this section, we first solve the special case of the studied problem when $M = 2, K = 1, f_w = 0, \Pr = 10, R = 3, \gamma = 1, G = 2$ and $\mathrm{Ec} = 0.02$ by RGT and EGT method with various α such as $-0.4, 0, 0.5, 1.5, 2.5$ and 3.5 and reporting the residual functions for different N in Table 1 while selecting $L = 4$ as the scaling factor. The residual functions by using Eq. (6) can be written as:

$$\begin{aligned}
\mathrm{Res}_1(\eta) &= f_N'''(\eta) + f_N(\eta) f_N''(\eta) - \left(f_N'(\eta)\right)^2 \\
&\quad - M f_N'(\eta) + K g_N'(\eta), \\
\mathrm{Res}_2(\eta) &= G g_N''(\eta) - (2 g_N(\eta) + f_N''), \\
\mathrm{Res}_3(\eta) &= \left(\frac{1+R}{R\mathrm{Pr}}\right)\theta_N''(\eta) + f_N(\eta)\theta_N'(\eta) \\
&\quad - \gamma f_N'(\eta)\theta_N(\eta) + \mathrm{Ec}(f_N''(\eta))^2,
\end{aligned} \tag{77}$$

and calculate $\|Res\|^2$ by means of

$$\|Res\|^2 = \int_0^\infty Res^2(\eta)\, d\eta. \tag{78}$$

According to this table, the downward trend of values of $\|\mathrm{Res}_1\|^2$, $\|\mathrm{Res}_2\|^2$ and $\|\mathrm{Res}_3\|^2$ by increasing N, indicates the fast convergence and good accuracy of the method for all cases of reported α. By investigation of the obtained values, it seems that the best interval for α is $(-0.5, 0.5]$ which $\alpha = 0$ has the better results. Based on this table and the absolute coefficients $|a_i|, |b_i|$ and $|c_i|$ of two categories of rational and exponential Gegenbauer functions are shown in Figs. 1, 2 and 3, it can be concluded that accurate solutions can be obtained by the implemented method even with small $N = 15$. So, we solve the rest of the cases of the problem by these parameters ($N = 15$, $\alpha = 0$ and $L = 4$) and report the residual values of the rational and the exponential Gegenbauer Tau method in Table 2.

The results in tables at expressed points $(f''(0), g'(0), \theta'(0))$ will be presented to investigate the behaviour of them for various parameters and compare them with the result of analytical (successive approximation) and numerical (shooting method) methods which reported in [57]. We know that $-f''(0)$, $g'(0)$ and $-\theta'(0)$ are the skin friction coefficient at the wall, wall couple stress and the local Nusselt number, respectively. So, we show the influences of parameter coupling constant on these criterions in Table 3. The two parameters that are

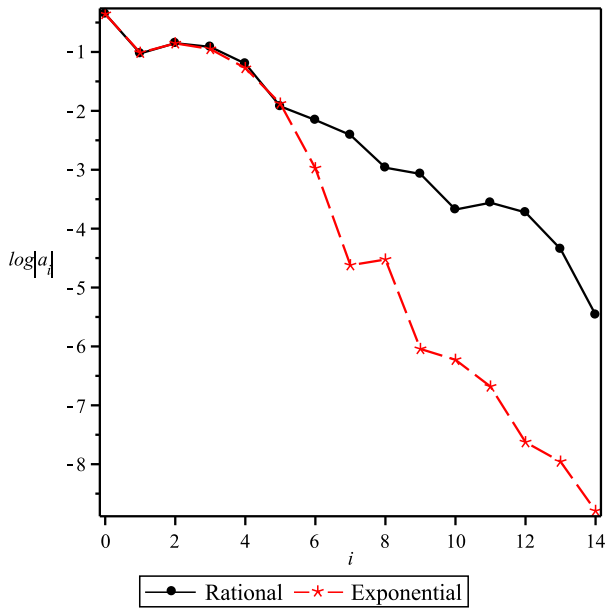

Fig. 1 Comparison between absolute coefficients $|a_i|$ of two categories of rational and exponential Gegenbauer functions when $M = 2, K = 1, f_w = 0, \Pr = 10, R = 3, \gamma = 1, G = 2, \mathrm{Ec} = 0.02$

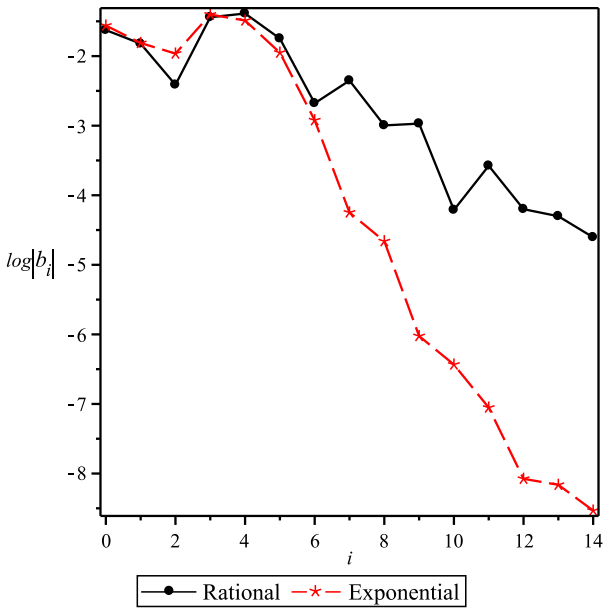

Fig. 2 Comparison between absolute coefficients $|b_i|$ of two categories of rational and exponential Gegenbauer functions when $M = 2, K = 1, f_w = 0, \Pr = 10, R = 3, \gamma = 1, G = 2, \mathrm{Ec} = 0.02$

directly related to the coupling rate are $-\theta'(0)$ and $g'(0)$, but the value of $-f''(0)$ is inversely related to the coupling rate.

Tables 4, 5 and 6 show that among the magnetic field, Prandtl number and radiation parameter, only the magnetic field affects the parameters of skin friction coefficient and wall couple stress whose values are increased by increasing the level of the magnetic field. This is expected since the linear and angular momentum equations [the first and the second equations in Eq. (6)] are uncoupled from the energy equation [the third equation in Eq. (6)] for this problem. Moreover, although increasing the Prandtl number and radiation parameter cause to increase the local Nusselt number, but this parameter decreases by the presence of the magnetic field.

The influence of the mass transfer parameter (f_w) is presented in Table 7. It shows that injection $(f_w \leq 0)$ reduces all three parameters mentioned above, but suction $(f_w > 0)$ increases them.

By considering obtained results in previous tables and figures, it is concluded that accuracy and convergency of EGT method is better for solving this problem. Also CPU time of solving the Eqs. (71)–(76) for RGT and EGT methods in Maple 18 software on a PC, CPU 2.2 GHz are presented in Table 8. With comparing the results it is concluded that EGT method is faster than RGT method for solving the problem. Therefore, for obtaining more results, EGT method was implemented.

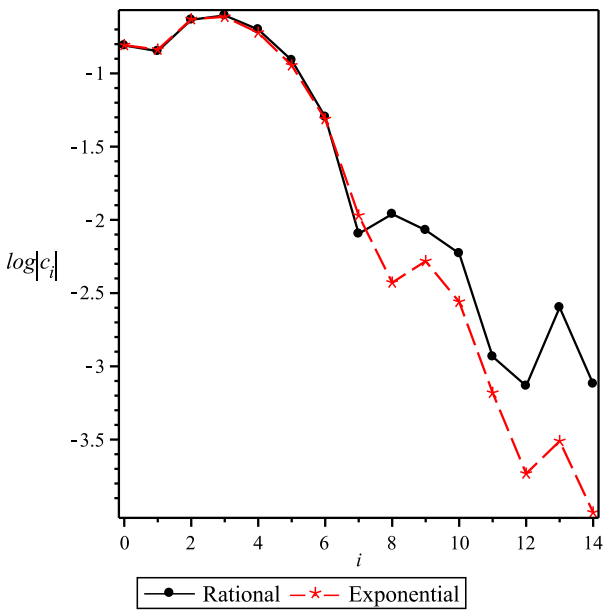

Fig. 3 Comparison between absolute coefficients $|c_i|$ of two categories of rational and exponential Gegenbauer functions when $M = 2, K = 1, f_w = 0, \Pr = 10, R = 3, \gamma = 1, G = 2, \mathrm{Ec} = 0.02$

In Figs. 4 and 5 the effect of the coupling parameter is considered and they show that by increasing K, $f'(\eta)$ decrease and $g(\eta)$ increases. Note that the velocity boundary layer thickness increased with increasing values

Table 2 The residual functions for three equations in main problem by using RGT and EGT methods when $\alpha = 0$ and $N = 15$

K	M	Pr	R	f_w	G	γ	Ec	RGT			EGT		
								$\|\text{Res}_1\|^2$	$\|\text{Res}_2\|^2$	$\|\text{Res}_3\|^2$	$\|\text{Res}_1\|^2$	$\|\text{Res}_2\|^2$	$\|\text{Res}_3\|^2$
1	2	10	3	0	2	1	0.02	5.94E−08	1.57E−08	1.87E−07	2.21E−17	8.99E−14	6.94E−09
4	2	10	3	0	2	1	0.02	3.95E−04	1.73E−06	1.93E−07	6.34E−10	4.26E−11	8.67E−09
1	1	10	3	0	2	1	0.02	9.25E−05	3.12E−07	7.89E−07	7.71E−13	5.32E−14	4.11E−08
1	3.8	10	3	0	2	1	0.02	2.32E−07	5.34E−10	1.64E−08	2.56E−16	4.10E−15	3.86E−10
1	2	0.71	3	0	2	1	0.02	5.94E−08	1.57E−08	1.93E−07	2.22E−17	7.26E−15	1.67E−07
1	2	5	3	0	2	1	0.02	5.94E−08	1.57E−08	4.58E−11	2.22E−17	7.26E−15	1.73E−11
1	2	10	0.1	0	2	1	0.02	5.94E−08	1.57E−08	1.00E−08	2.22E−17	7.26E−15	1.08E−13
1	2	10	0.5	0	2	1	0.02	5.94E−08	1.57E−08	3.91E−11	2.22E−17	7.26E−15	3.45E−12
1	2	10	1	0	2	1	0.02	5.94E−08	1.57E−08	4.11E−09	2.22E−17	7.26E−15	4.82E−10
1	2	10	3	−0.5	2	1	0.02	3.94E−05	2.33E−07	7.50E−10	2.82E−08	7.08E−12	3.27E−12
1	2	10	3	0.5	2	1	0.02	6.54E−06	1.63E−08	1.64E−06	2.46E−08	4.93E−12	3.86E−07

Table 3 Comparison between RGT and EGT methods with results of [57] for $f''(0), g'(0)$ and $\theta'(0)$ by various K when $M = 2, f_w = 0, \text{Pr} = 10, R = 3, \gamma = 1, G = 2, \text{Ec} = 0.02$

K	Analytical [57]	Numerical [57]	RGT	EGT
	$f''(0)$			
1	− 1.676622	− 1.676305	− 1.676350	− 1.676305
4	− 1.493959	− 1.494670	− 1.498385	− 1.494670
	$g'(0)$			
1	0.310602	0.317949	0.317946	0.317949
4	0.325028	0.321999	0.321966	0.321999
	$\theta'(0)$			
1	− 2.933228	− 2.932841	− 2.928977	− 2.932825
4	− 2.973965	− 2.974663	− 2.960146	− 2.965177

Table 4 Comparison between RGT and EGT methods with results of [57] for $f''(0), g'(0)$ and $\theta'(0)$ by various M when $K = 1, f_w = 0, \text{Pr} = 10, R = 3, \gamma = 1, G = 2, \text{Ec} = 0.02$

M	Analytical [57]	Numerical [57]	RGT	EGT
	$f''(0)$			
1	− 1.358082	− 1.358217	− 1.360011	− 1.358217
2	− 1.676622	− 1.676305	− 1.676350	− 1.676305
3.8	− 2.138957	− 2.138018	− 2.137928	− 2.138018
	$g'(0)$			
1	0.283562	0.294877	0.294868	0.294877
2	0.310602	0.317949	0.317946	0.317949
3.8	0.339333	0.343713	0.343713	0.343713
	$\theta'(0)$			
1	− 3.033721	− 3.034414	− 3.027976	− 3.034371
2	− 2.933228	− 2.932841	− 2.928977	− 2.932825
3.8	− 2.779171	− 2.779855	− 2.779873	− 2.781256

Table 5 Comparison between RGT and EGT methods with results of [57] for $f''(0), g'(0)$ and $\theta'(0)$ by various Pr when $M = 2, K = 1, f_w = 0, R = 3, \gamma = 1, G = 2, \text{Ec} = 0.02$

Pr	Analytical [57]	Numerical [57]	RGT	EGT
	$f''(0)$			
0.71	− 1.676622	− 1.676305	− 1.676350	− 1.676305
5	− 1.676622	− 1.676305	− 1.676350	− 1.676305
10	− 1.676622	− 1.676305	− 1.676350	− 1.676305
	$g'(0)$			
0.71	0.310602	0.317949	0.317946	0.317949
5	0.310602	0.317949	0.317946	0.317949
10	0.310602	0.317949	0.317946	0.317949
	$\theta'(0)$			
0.71	− 0.507583	− 0.500570	− 0.478292	− 0.478260
5	− 1.948456	− 1.949998	− 1.949977	− 1.949998
10	− 2.933228	− 2.932841	− 2.928977	− 2.932825

of K associated with the decrease in the wall velocity gradient. The relationship between the coupling parameter and the temperature profile is straightforward, but due to the slight increase in $\theta(\eta)$ with increasing coupling, we have not drawn its figure. The desired functions (fluid velocity, angular-velocity and temperature profile) are influenced by the magnetic field whose figures are shown in Figs. 6, 7 and 8, respectively. With the presence of a magnetic field, the flow face to a drag-like force, namely the Lorentz force whose action is opposite to the direction of the fluid motion and causes to decreasing the fluid velocity and angular-velocity but instead increasing the fluid temperature. The velocity boundary layer thickness decreases while the thermal boundary layer thickness increases as M increases. In addition, the maximum of the

Table 6 Comparison between RGT and EGT methods with results of [57] for $f''(0), g'(0)$ and $\theta'(0)$ by various R when $M = 2, K = 1, f_w = 0, \Pr = 10, \gamma = 1, G = 2, \mathrm{Ec} = 0.02$

R	Analytical [57]	Numerical [57]	RGT	EGT
	$f''(0)$			
0.1	− 1.676622	− 1.676305	− 1.676350	− 1.676305
0.5	− 1.676622	− 1.676305	− 1.676350	− 1.676305
1	− 1.676622	− 1.676305	− 1.676350	− 1.676305
3	− 1.676622	− 1.676305	− 1.676350	− 1.676305
	$g'(0)$			
0.1	0.310602	0.317949	0.317946	0.317949
0.5	0.310602	0.317949	0.317946	0.317949
1	0.310602	0.317949	0.317946	0.317949
3	0.310602	0.317949	0.317946	0.317949
	$\theta'(0)$			
0.1	− 0.719536	− 0.742685	− 0.737100	− 0.737100
0.5	− 1.807747	− 1.813284	− 1.813271	− 1.813283
1	− 2.317869	− 2.318467	− 2.318089	− 2.318462
3	− 2.933228	− 2.932841	− 2.928977	− 2.932825

angular velocity decreases in amplitude and the location of the maximum velocity moves closer to the wall with an increase of M. According to the tables, the Prandtl number and radiation parameter just effects with inversely related on temperature profile $\theta(\eta)$, Figs. 9 and 10, respectively. As the Prandtl increases, there is a fall in the fluid temperature as well as its boundary layer thickness. This causes the wall slope of the temperature profile to decrease as Pr increases, causing the Nusselt number to increase as clearly was shown in Table 5. It should be noted that when $R \to \infty$, we are facing a condition where thermal radiation effect is absent. This indicates that as the parameter R increases, thermal radiation effects become lower and this means that the temperature decreases and the negative slope of the temperature profile at the surface increases as shown in Table 5. At last, different mass transfer f_w considered and the effect of this parameter on three desired profiles as $f'(\eta)$, $g(\eta)$ and $\theta(\eta)$ and illustrated in Figs. 11, 12 and 13, respectively, which show that suction leads to decrease all profiles and injection leading to opposite behaviour. Applying suction at the stretching surface causes to draw the amount of the fluid into the surface and consequently the hydrodynamic boundary layer thickness decreases. If $(f_w > 0)$, high resistance afford by the fluid and has a tendency to reduce the velocity of the flow, but wall injection $(f_w \leq 0)$ produces the opposite effect. Also, the thermal boundary layer gets depressed by increasing the suction parameter. Therefore, for increasing the value of f_w, the temperature field gradually decreases.

Table 8 The computer run time of RGT and EGT methods in second when $N = 15$

K	M	Pr	R	f_w	G	γ	Ec	RGT (s)	EGT (s)
1	2	10	3	0	2	1	0.02	2.293	1.408
4	2	10	3	0	2	1	0.02	2.543	1.482
1	1	10	3	0	2	1	0.02	2.580	1.482
1	3.8	10	3	0	2	1	0.02	1.638	1.436
1	2	0.71	3	0	2	1	0.02	2.231	1.778
1	2	5	3	0	2	1	0.02	2.481	1.950
1	2	10	0.1	0	2	1	0.02	2.652	2.059
1	2	10	0.5	0	2	1	0.02	2.636	2.106
1	2	10	1	0	2	1	0.02	2.605	2.091
1	2	10	3	− 0.5	2	1	0.02	2.371	1.966
1	2	10	3	0.5	2	1	0.02	3.136	2.858

Table 7 Comparison between RGT and EGT methods with results of [57] for $f''(0), g'(0)$ and $\theta'(0)$ by various f_w when $M = 2, K = 1, \Pr = 10, R = 3, \gamma = 1, G = 2, \mathrm{Ec} = 0.02$

f_w	Analytical [57]	Numerical [57]	RGT	EGT
	$f''(0)$			
− 0.5	− 1.434341	− 1.444333	− 1.445684	− 1.444294
0	− 1.676622	− 1.676305	− 1.676350	− 1.676305
0.5	− 1.940262	− 1.946052	− 1.945493	− 1.946015
	$g'(0)$			
− 0.5	0.292893	0.300334	0.300312	0.300334
0	0.310602	0.317949	0.317946	0.317949
0.5	0.327805	0.334831	0.334828	0.334831
	$\theta'(0)$			
− 0.5	− 1.398473	− 1.392094	− 1.392090	− 1.392087
0	− 2.933228	− 2.932841	− 2.928977	− 2.932825
0.5	− 5.528042	− 5.527730	− 5.558338	− 5.526077

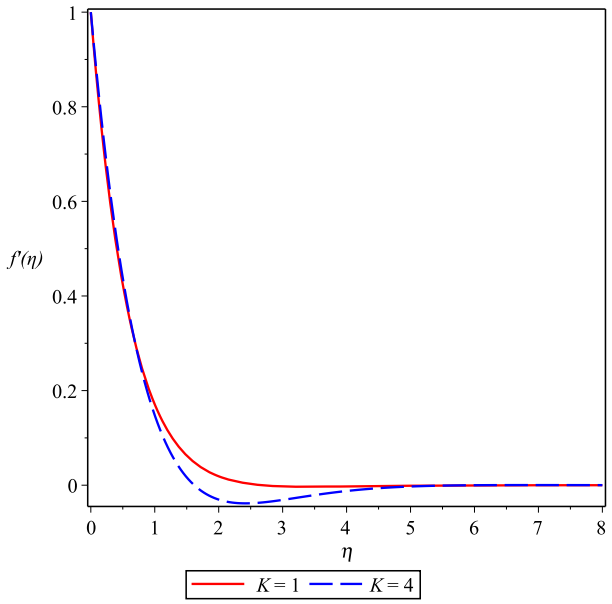

Fig. 4 Velocity profile-dependence of coupling constant parameter K, when $M = 2, f_w = 0, \mathrm{Pr} = 10, R = 3, \gamma = 1, G = 2, \mathrm{Ec} = 0.02$

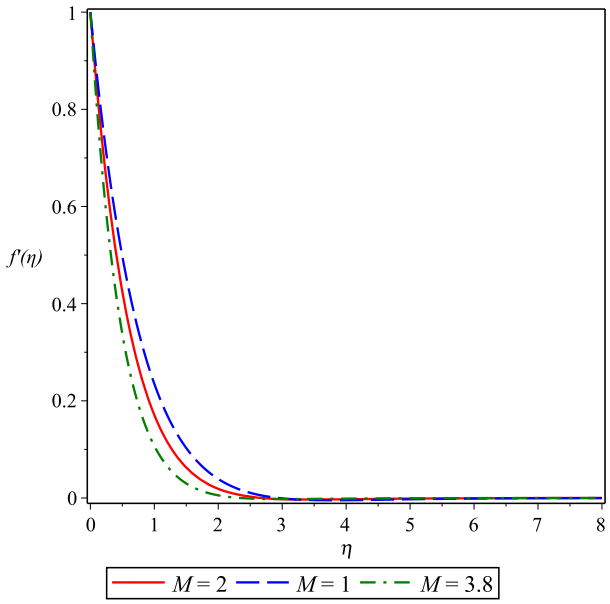

Fig. 6 Velocity profile-dependence of magnetic parameter M, when $K = 1, f_w = 0, \mathrm{Pr} = 10, R = 3, \gamma = 1, G = 2, \mathrm{Ec} = 0.02$

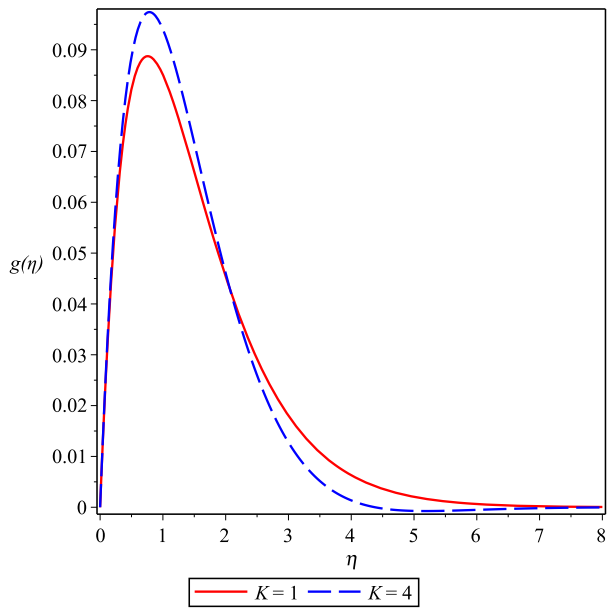

Fig. 5 Angular velocity profile-dependence of coupling constant parameter K, when $M = 2, f_w = 0, \mathrm{Pr} = 10, R = 3, \gamma = 1, G = 2, \mathrm{Ec} = 0.02$

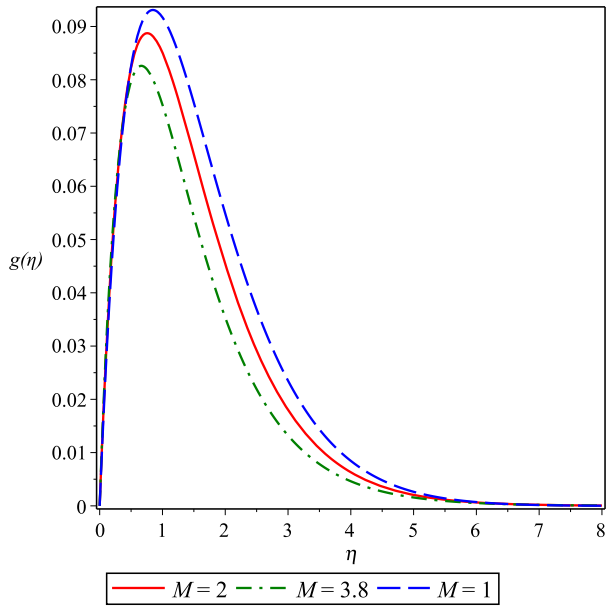

Fig. 7 Angular Velocity profile-dependence of magnetic parameter M, when $K = 1, f_w = 0, \mathrm{Pr} = 10, R = 3, \gamma = 1, G = 2, \mathrm{Ec} = 0.02$

8 Conclusions

In this paper, a numerical approach called Tau method has been implemented to solve the system of coupled nonlinear ordinary differential equations. The fluid flow consists a MHD micropolar fluid which past a moving plate with suction and injection boundary conditions with considering heat transfer. In this research, two different functions were used; rational and exponential Gegenbauer functions. For solving the system of equations basis functions of Tau method was implemented. To the best of our knowledge, this is the first time that the derivative matrices of these functions were introduced and applied to Tau method for

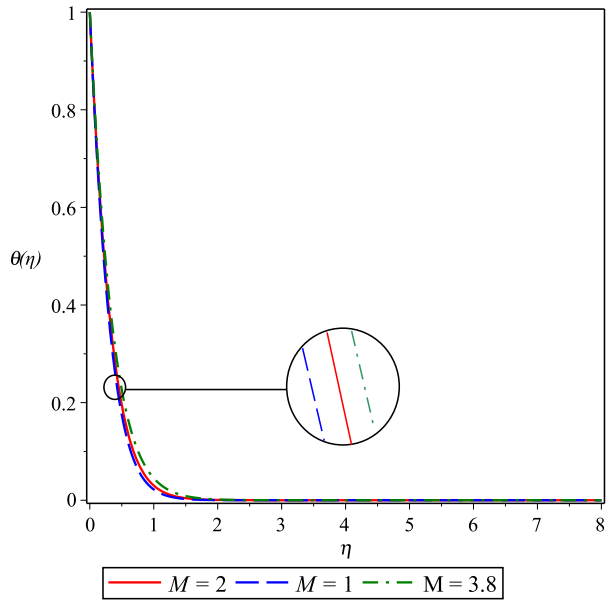

Fig. 8 Temperature profile-dependence of magnetic parameter M, when $K = 1, f_w = 0, \Pr = 10, R = 3, \gamma = 1, G = 2, \mathrm{Ec} = 0.02$

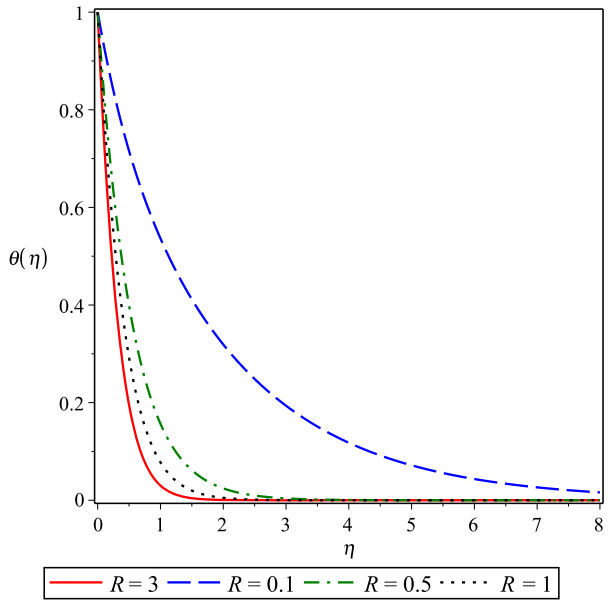

Fig. 10 Temperature profile-dependence of radiation parameter R, when $M = 2, K = 1, f_w = 0, \Pr = 10, \gamma = 1, G = 2, \mathrm{Ec} = 0.02$

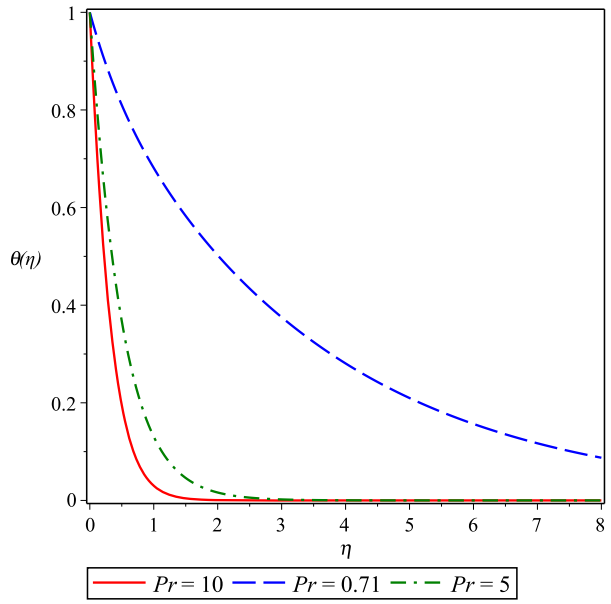

Fig. 9 Temperature profile-dependence of Prandtl number Pr, when $M = 2, K = 1, f_w = 0, R = 3, \gamma = 1, G = 2, \mathrm{Ec} = 0.02$

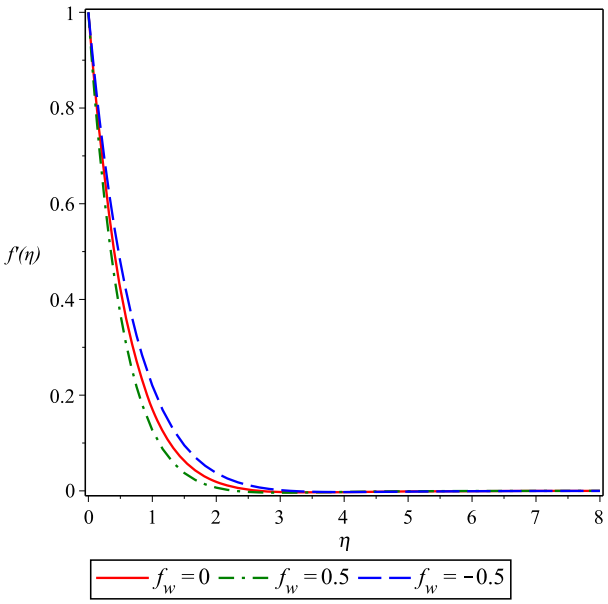

Fig. 11 Velocity profile-dependence of mass transfer parameter f_w, when $M = 2, K = 1, \Pr = 10, R = 3, \gamma = 1, G = 2, \mathrm{Ec} = 0.02$

solving a complicated heat and mass transfer phenomena. Also, the exponential convergence rate of approximation of the analytical functions by these basis functions was discussed in this paper. In the numerical result section, the effects of some important physical parameters of the system were discussed through tables and graphs. According to the good stability and convergence rate of Tau method, it can be used for solving similar problem, also it should be mentioned that the considered computational domain is infinite and this proves that this method has a good ability for solving boundary layer problems, such as the solved problem by considering the induced magnetic field and the

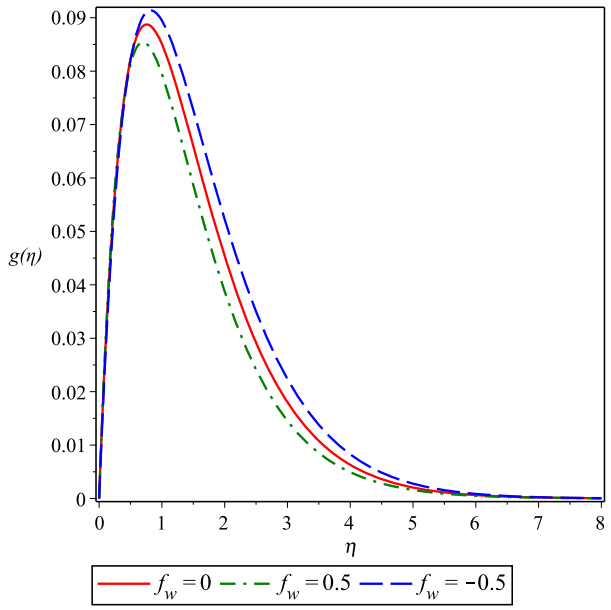

Fig. 12 Angular velocity profile-dependence of mass transfer parameter f_w, when $M = 2, K = 1, \Pr = 10, R = 3, \gamma = 1, G = 2, \mathrm{Ec} = 0.02$

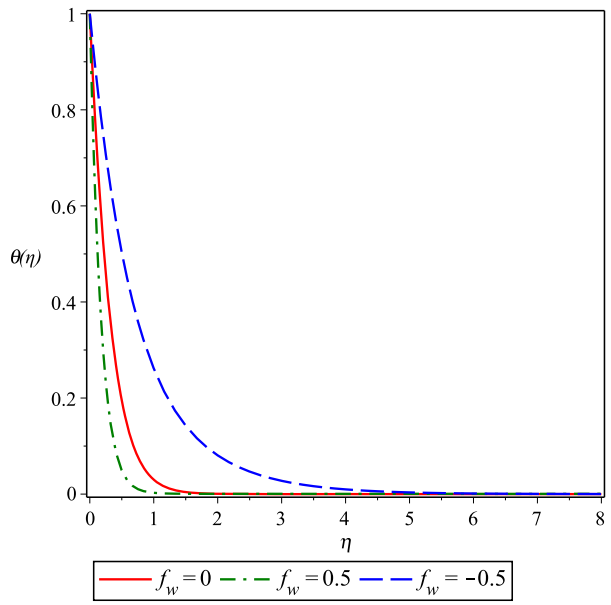

Fig. 13 Temperature profile-dependence of mass transfer parameter f_w, when $M = 2, K = 1, \Pr = 10, R = 3, \gamma = 1, G = 2, \mathrm{Ec} = 0.02$

Hall effect are included. The obtained results have excellent agreement with the approximate and exact solution. Although both introduced basis functions have provided an acceptable result for this equation in Tau method, according to the residual functions, it seems that the accuracy and speed convergence of the exponential Gegenbauer Tau method is much better for solving this problem. At last, we note that the introduced methods can be applied even for the PDEs system as well as fractional PDEs by expanding the multi-variable functions and using the operational matrices to obtain partial derivatives and the residual functions.

Acknowledgements The authors are very grateful to both reviewers for carefully reading this paper and for their comments and suggestions which have improved the paper.

References

1. Canuto C, Hussaini MY, Quarteroni A, Zang TA (1986) Spectral methods in fluid dynamics. Prentice-Hall, Englewood Cliffs
2. Assari P, Dehghan M (2017) The numerical solution of two-dimensional logarithmic integral equations on normal domains using radial basis functions with polynomial precision. Eng Comput 33(4):853–870
3. Khalil H, Khan RA, Baleanu D, Rashidi MM (2019) Some new operational matrices and its application to fractional order Poisson equations with integral type boundary constrains. Comput Math Appl 78(6):1826–1837
4. Hosseininia M, Heydari MH, Ghaini FMM, Avazzadeh Z (2019) A wavelet method to solve nonlinear variable-order time fractional 2D Klein–Gordon equation. Comput Math Appl 78(12):3713–3730
5. Lanczos C (1938) Trigonometric interpolation of empirical and analytical functions. J Math Phys 17:123–199
6. Tajvidi T, Razzaghi M, Dehghan M (2008) Modified rational Legendre approach to laminar viscous flow over a semi-infinite flat plate. Chaos Solitons Fractals 35:59–66
7. El-Daou MK (2011) Exponentially weighted Legendre–Gauss Tau methods for linear second-order differential equations. Comput Math Appl 62:51–64
8. Saadatmandi A, Dehghan M (2011) A Tau approach for solution of the space fractional diffusion equation. Comput Math Appl 62:1135–1142
9. Doha EH, Bhrawy AH, Ezz-Eldien SS (2011) Efficient Chebyshev spectral methods for solving multi-term fractional orders differential equations. Appl Math Model 35:5662–5672
10. Coulaud O, Funaro D, Kavian O (1990) Laguerre spectral approximation of elliptic problems in exterior domains. Comput Method Appl Mech Eng 80:451–458
11. Funaro D, Kavian O (1991) Approximation of some diffusion evolution equations in unbounded domains by Hermite functions. Math Comput 57:597–619
12. Liu C, Zhub S (2015) Laguerre pseudospectral approximation to the Thomas–Fermi equation. J Comput Appl Math 282:251–261
13. Alıcı H, Taşeli H (2015) The Laguerre pseudospectral method for the radial Schrödinger equation. Appl Numer Math 87:87–99
14. Guo BY (2000) Jacobi spectral approximation and its applications to differential equations on the half line. J Comput Math 18:95–112
15. Guo BY (2001) Gegenbauer approximation and its applications to differential equations with rough asymptotic behaviors at infinity. Appl Numer Math 38:403–425
16. Boyd JP (2000) Chebyshev and Fourier spectral methods, 2nd edn. Dover, New York
17. Christov CI (1982) A complete orthogonal system of functions in $L^2(-\infty, \infty)$ space. SIAM J Appl Math 42:1337–1344
18. Boyd JP (1987) Orthogonal rational functions on a semi-infinite interval. J Comput Phys 70:63–88

19. Boyd JP (1987) Spectral methods using rational basis functions on an infinite interval. J Comput Phys 69:112–142
20. Guo BY, Shen J, Wang ZQ (2000) A rational approximation and its applications to differential equations on the half line. J Sci Comput 15:117–147
21. Boyd JP, Rangan C, Bucksbaum PH (2003) Pseudospectral methods on a semi-infinite interval with application to the Hydrogen atom: a comparison of the mapped Fourier-sine method with Laguerre series and rational Chebyshev expansions. J Comput Phys 188:56–74
22. Parand K, Razzaghi M (2004) Rational Chebyshev Tau method for solving higher-order ordinary differential equations. Int J Comput Math 81:73–80
23. Parand K, Razzaghi M (2004) Rational Chebyshev Tau method for solving Volterra's population model. Appl Math Comput 149:893–900
24. Parand K, Dehghan M, Rezaei AR, Ghaderi SM (2010) An approximational algorithm for the solution of the nonlinear Lane–Emden type equations arising in astrophysics using Hermite functions collocation method. Comput Phys Commun 181:1096–1108
25. Parand K, Dehghan M, Taghavi A (2010) Modified generalized Laguerre function Tau method for solving laminar viscous flow: the Blasius equation. Int J Numer Methods Heat Fluid Flow 20:728–743
26. Parand K, Nikarya M, Rad JA, Baharifard F (2012) A new reliable numerical algorithm based on the first kind of Bessel functions to solve Prandtl–Blasius laminar viscous flow over a semi-infinite flat plate. Z Naturforsch A 67:665–673
27. Parand K, Dehghan M, Baharifard F (2013) Solving a laminar boundary layer equation with the rational Gegenbauer functions. Appl Math Model 37:851–863
28. Baharifard F, Kazem S, Parand K (2015) Rational and exponential legendre Tau method on steady flow of a third grade fluid in a porous half space. Int J Appl Comput Math 67:1–20
29. Rabiei K, Parand K (2019) Collocation method to solve inequality-constrained optimal control problems of arbitrary order. Eng Comput 36:1–11
30. Gudi T, Majumder P (2019) Conforming and discontinuous Galerkin FEM in space for solving parabolic obstacle problem. Comput Math Appl 78(12):3896–3915
31. Modather M, Chamkha AJ (2010) An analytical study of MHD heat and mass transfer oscillatory flow of a micropolar fluid over a vertical permeable plate in a porous medium. Turk J Eng Environ Sci 33(4):245–258
32. Damseh RA, Al-Odat MQ, Chamkha AJ, Shannak BA (2009) Combined effect of heat generation or absorption and first-order chemical reaction on micropolar fluid flows over a uniformly stretched permeable surface. Int J Therm Sci 48(8):1658–1663
33. Eringen AC (1966) Theory of micropolar fluids. J Math Mech 16:1–18
34. Eringen AC (2001) Microcontinuum field theories: II. Fluent media. Springer, New York
35. Łukaszewicz G (1999) Micropolar fluids, theory and applications, modeling and simulation in science, engineering and technology. Birkhäuser, Boston
36. Ariman T, Turk MA, Sylvester ND (1974) Microcontinuum fluid mechanics—a review. Int J Eng Sci 12:273–293
37. Sakiadis BC (1961) Boundary layer behavior on continuous solid surface; the boundary layer on a continuous flat surface. Am Inst Chem Eng J 7:221–225
38. Soundalgekar VM, Takhar HS (1983) Boundary layer flow of a micropolar fluid on a continuous moving plate. Int J Eng Sci 21:961–965
39. Crane LJ (1970) Flow past a stretching plate. Z Angew Math Phys 21:645–647
40. Abolbashari MH, Freidoonimehr N, Nazari F, Rashidi MM (2014) Entropy analysis for an unsteady MHD flow past a stretching permeable surface in nano-fluid. Powder Technol 267:256–267
41. Freidoonimehr N, Rashidi MM, Mahmud S (2015) Unsteady MHD free convective flow past a permeable stretching vertical surface in a nano-fluid. Int J Threm Sci 87:136–145
42. Chamkha AJ, Aly AM, Mansour MA (2010) Similarity solution for unsteady heat and mass transfer from a stretching surface embedded in a porous medium with suction/injection and chemical reaction effects. Chem Eng Commun 197(6):846–858
43. Rees DAS, Bassom AP (1996) The Blasius boundary-layer flow of a micropolar fluid. Int J Eng Sci 34:113–124
44. Gupta P, Gupta A (1977) Heat and mass transfer on a stretching sheet with suction or blowing. Can J Chem Eng 55:744–746
45. Hassanien IA, Gorla RSR (1990) Heat transfer to a micropolar fluid from a nonisothermal stretching sheet with suction and blowing. Acta Mech 84:191–203
46. Hady FM (1996) On the solution of heat transfer to micropolar fluid from a nonisothermal stretching sheet with injection. Int J Numer Meth Heat Fluid Flow 6:99–104
47. Perdikis C, Raptis A (1996) Heat transfer of a micropolar fluid by the presence of radiation. Heat Mass Transf 31:381–382
48. Raptis A (1998) Flow of a micropolar fluid past a continuously moving plate by the presence of radiation. Int J Heat Mass Transf 41:2865–2866
49. Chamkha AJ (2002) Fully developed free convection of a micropolar fluid in a vertical channel. Int Commun Heat Mass Transf 29:1119–1127
50. Rahman MM, Uddin MJ, Aziz A (2009) Effects of variable electric conductivity and non-uniform heat source (or sink) on convective micropolar fluid flow along an inclined flat plate with surface heat flux. Int J Therm Sci 48:2331–2340
51. Zhang J-K, Li B-W, Hu Z-M (2013) Effects of optical parameters on fluid flow and heat transfer of participating magnetic fluid. Int J Heat Mass Transf 59:126–136
52. Magyari E, Chamkha AJ (2008) Exact analytical results for the thermosolutal MHD Marangoni boundary layers. Int J Therm Sci 47(7):848–857
53. Takhar HS, Chamkha AJ, Nath G (2002) MHD flow over a moving plate in a rotating fluid with magnetic field, Hall currents and free stream velocity. Int J Eng 40(13):1511–152
54. Takhar HS, Chamkha AJ, Nath G (1999) Unsteady flow and heat transfer on a semi-infinite flat plate with an aligned magnetic field. Int J Eng 37(13):1723–1736
55. Chamkha AJ, Aly AM (2010) MHD free convection flow of a nanofluid past a vertical plate in the presence of heat generation or absorption effects. Chem Eng Commun 198(3):425–441
56. Seddeek MA (2003) Flow of a magneto-micropolar fluid past a continuously moving plate. Phys Lett A 306:255–257
57. Seddeek MA, Odda SN, Akl MY, Abdelmeguid MS (2009) Analytical solution for the effect of radiation on flow of a magneto-micropolar fluid past a continuously moving plate with suction and blowing. Comput Mater Sci 45:423–428
58. Khedr MEM, Chamkha AJ, Bayomi M (2009) MHD flow of a micropolar fluid past a stretched permeable surface with heat generation or absorption. Nonlinear Anal Model 14(1):27–40
59. Chamkha AJ, Mohamed RA, Ahmed SE (2011) Unsteady MHD natural convection from a heated vertical porous plate in a micropolar fluid with Joule heating, chemical reaction and radiation effects. Meccanica 46(2):399–411
60. Bhargava R, Bég OA, Sharma S, Zueco J (2010) Finite element study of nonlinear two-dimensional deoxygenated biomagnetic micropolar flow. Commun Nonlinear Sci 15(5):1210–1223
61. Aslani KE, Benos L, Tzirtzilakis E, Sarris IE (2020) Micro-magnetorotation of MHD micropolar flows. Symmetry 12:1

62. Rashidi MM, Erfani E (2012) Analytical method for solving steady MHD convective and slip flow due to a rotating disk with viscous dissipation and ohmic heating. Eng Comput 6:562–579
63. Rashidi MM, Momoniat E, Rostami B (2012) Analytic approximate solutions for MHD boundary-layer viscoelastic fluid flow over continuously moving stretching surface by homotopy analysis method with two auxiliary parameters. J Appl Math 2012:1–19
64. Raptis A, Perdikis C, Takhar HS (2004) Effect of thermal radiation on MHD flow. Appl Math Comput 153:645–649
65. Szegö G (1975) Orthogonal polynomials, 4th edn. AMS Coll Publ, New York
66. Stegun I, Abramowitz M (1968) Handbook of mathematical functions. Dover, New York
67. Boyd JP (1982) The optimzation of convergence for Chebyshev polynomial methods in an unbounded domain. J Comput Phys 45:43–79
68. Kim DS, Kim T, Rim SH (2012) Some identities involving Gegenbauer polynomials. Adv Differ Equ 2012:219